

The *C. elegans* hox gene *lin-39* controls cell cycle progression during vulval development

Journal Article**Author(s):**

Roiz, Daniel; Escobar-Restrepo, Juan Miguel; Leu, Philipp; Hajnal, Alex

Publication date:

2016-10

Permanent link:

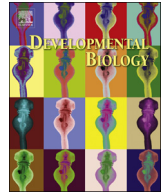
<https://doi.org/https://doi.org/10.3929/ethz-b-000121358>

Rights / license:

[Creative Commons Attribution-NonCommercial-NoDerivatives 4.0 International](#)

Originally published in:

Developmental Biology 418(1), <https://doi.org/10.1016/j.ydbio.2016.07.018>



The *C. elegans* *hox* gene *lin-39* controls cell cycle progression during vulval development



Daniel Roiz^{a,b}, Juan Miguel Escobar-Restrepo^a, Philipp Leu^{a,1}, Alex Hajnal^{a,*}

^a Institute of Molecular Life Sciences, University of Zurich, Zurich, Switzerland

^b Molecular Life Science PhD Program, University and ETH Zurich, Zurich, Switzerland

ARTICLE INFO

Article history:

Received 5 March 2016

Received in revised form

12 July 2016

Accepted 19 July 2016

Available online 27 July 2016

Keywords:

C. elegans

Vulval development

hox gene

NOTCH

Cyclin

Cyclin-dependent kinase, proliferation

ABSTRACT

Cell fate specification during organogenesis is usually followed by a phase of cell proliferation to produce the required number of differentiated cells. The *Caenorhabditis elegans* vulva is an excellent model to study how cell fate specification and cell proliferation are coordinated. The six vulval precursor cells (VPCs) are born at the first larval stage, but they arrest in the G1 phase of the cell cycle until the beginning of the third larval stage, when their fates are specified and the three proximal VPCs proliferate to generate 22 vulval cells. An epidermal growth factor (EGF) signal from the gonadal anchor cell combined with lateral DELTA/NOTCH signaling between the VPCs determine the primary (1°) and secondary (2°) fates, respectively. The *hox* gene *lin-39* plays a key role in integrating these spatial patterning signals and in maintaining the VPCs as polarized epithelial cells. Using a fusion-defective *eff-1(lf)* mutation to keep the VPCs polarized, we find that VPCs lacking *lin-39* can neither activate lateral NOTCH signaling nor proliferate. LIN-39 promotes cell cycle progression through two distinct mechanisms. First, LIN-39 maintains the VPCs competent to proliferate by inducing *cdk-4 cdk* and *cye-1 cyclinE* expression via a non-canonical HOX binding motif. Second, LIN-39 activates in the adjacent VPCs the NOTCH signaling pathway, which promotes VPC proliferation independently of LIN-39. The *hox* gene *lin-39* is therefore a central node in a regulatory network coordinating VPC differentiation and proliferation.

© 2016 The Authors. Published by Elsevier Inc. This is an open access article under the CC BY-NC-ND license (<http://creativecommons.org/licenses/by-nc-nd/4.0/>).

1. Introduction

During organogenesis, two-dimensional sheets of epithelial cells are remodeled into three-dimensional organs (Trinkaus, 1984). This process is guided by soluble and membrane-associated ligand-receptor interactions that activate intracellular signaling pathways, which in turn control nuclear determinants such as *Hox*, *ETS*, *ZnF*, *bHLH* or *Forkhead* transcription factors. Organogenesis can be divided into four conceptual steps that are compartmentalized in time: (1) specification of the precursor cells that are competent to differentiate, (2) induction of distinct cell fates among the precursor cells, (3) proliferation of the precursor cells to generate the required number of cells of the different types and (4) terminal differentiation and spatial rearrangement of post-mitotic cells during the morphogenesis phase. However, we currently lack a clear understanding of the mechanisms that coordinate these different steps of organogenesis.

The *hox* genes encode homeobox domain-containing

transcription factors that play diverse roles during organogenesis (Rezsohazy et al., 2015). Originally discovered as the determinants of segment identity in the *Drosophila* embryo (Lewis, 1978), *hox* genes control a broad range of cellular functions including cell proliferation and tissue morphogenesis. Moreover, de-regulated expression of *hox* genes has also been linked to the formation of acute myeloid (AML) and lymphoid leukemia (ALL) in humans (Celetti et al., 1993; Soulier et al., 2005). HOX proteins form heterodimers with their PBX or MEIS family co-factors to activate target genes that carry distinct DNA motifs in their enhancers (Rezsohazy et al., 2015). However, there exists no comprehensive picture of the direct *hox* target genes that mediate the different aspects of *hox* gene function.

The development of the *Caenorhabditis elegans* vulva, the egg-laying organ of the hermaphrodite, is an excellent model to investigate how cell fate specification, cell proliferation and organ morphogenesis are coordinated in time and space (reviewed by Schindler and Sherwood (2012), Schmid and Hajnal (2015) and Sternberg (2005)). Vulval fate specification involves the combined action of the conserved Wingless (WNT), EGFR/RAS/MAPK and DELTA/NOTCH signaling pathways. Towards the end of the first larval stage (L1), twelve epidermal Pn.p cells align along the ventral midline of the animal. A WNT signal from a group of tail

* Corresponding author.

E-mail address: alex.hajnal@imls.uzh.ch (A. Hajnal).

¹ Current address: Institute of Biochemistry, ETH Zurich, Switzerland.

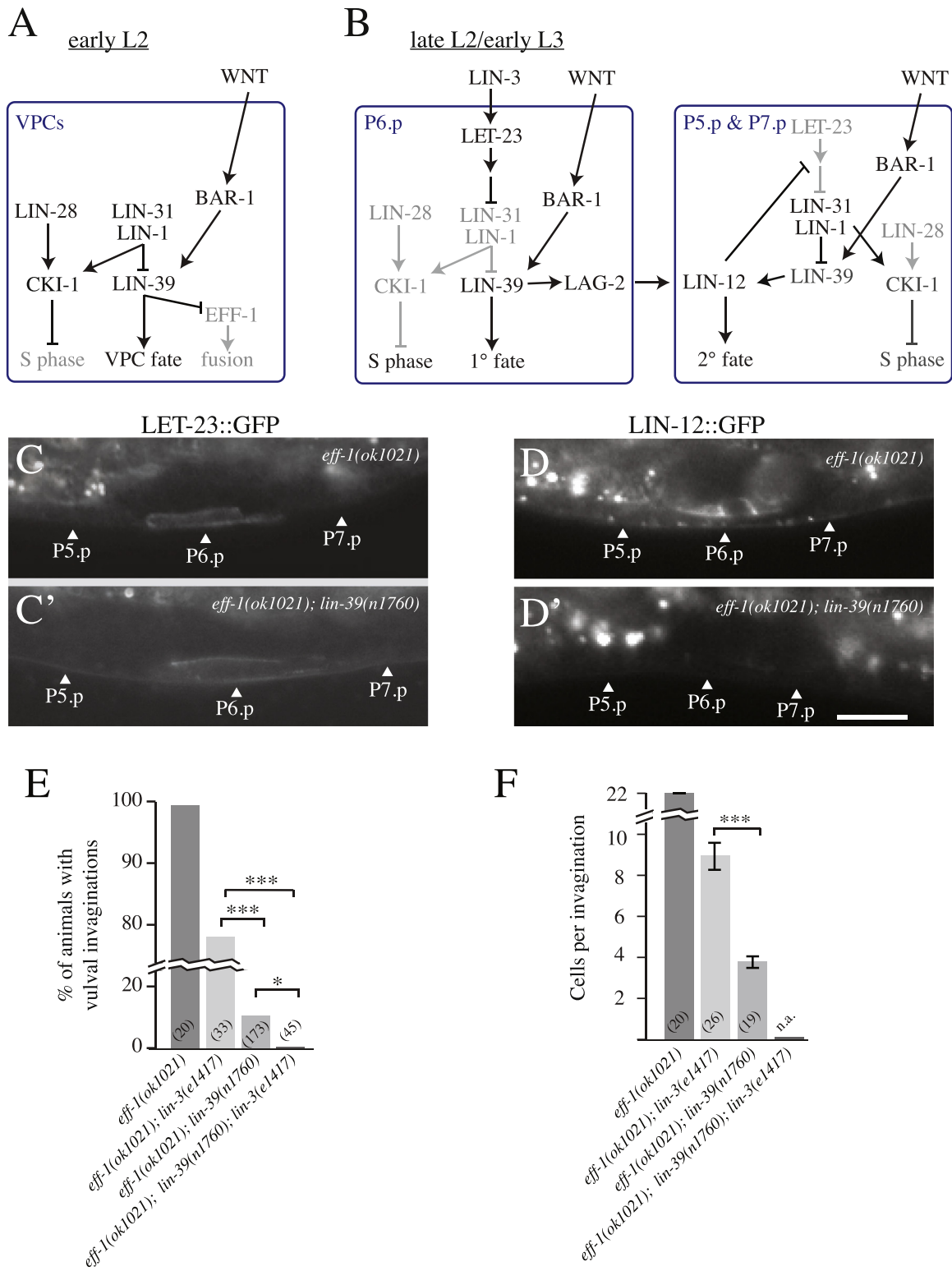


Fig. 1. The VPCs in *lin-39* mutants are partially sensitive to the inductive AC signal but do not proliferate. (A) Signaling pathways and transcription factor network controlling VPC differentiation and proliferation. During the L2 stage, Wnt signaling maintains basal LIN-39 levels, while LIN-31 and LIN-1 repress *lin-39* transcription. The heterochronic LIN-28 protein as well as LIN-31 activate *cki-1* expression to arrest the VPCs in the G1 phase of the cell cycle. (B) Towards the end of the L2 stage, the inductive LIN-3 EGF signal activates the LET-23 EGFR pathway in the 1° VPC (P6.p), resulting in the inactivation of the LIN-1/LIN-31 complex towards MAPK phosphorylation. Together with the fading in LIN-28 levels, this causes a reduction in CKI-1 expression, permitting the VPCs to enter S-phase. At the same time, elevated LIN-39 levels activate LAG-2 expression to induce lateral LIN-12 NOTCH signaling in the adjacent 2° VPCs (P5.p & P7.p). LIN-12 NOTCH signaling then inhibits LET-23 signaling and induces the 2° vulval fate. (C) Expression of a functional LET-23::GFP reporter in P6.p of an *eff-1(lf)* single and (C') an *eff-1(lf); lin-39(n1760)* double mutant at the late L2/early L3 stage. (D) Expression of a functional LIN-12::GFP reporter on the apical membranes of P5.p through P7.p in an *eff-1(lf)* single mutant and (D') loss of LIN-12::GFP expression in an *eff-1(lf); lin-39(n1760)* double mutant. (E) Vulval invaginations in *lin-39(lf)* mutants require the inductive LIN-3 signal. For each genotype, the percentage of animals developing a vulval invagination and (F) the average number of cells per invagination in those animals that formed an invagination are shown (e.g. in 18 out of the 173 *eff-1(lf); lin-39(n1760)* double mutants analyzed). The number of animals analyzed for each genotype is shown in brackets. The error bars represent the standard error of the mean (s.e.m.). Statistical significance was analyzed with a Fisher's exact probability test; * signifies $p < 0.05$ and *** $p < 0.001$.

cells induces the expression of the *hox* gene *lin-39* in six Pn.p cells in the mid-body region (P3.p through P8.p), which become the vulval precursor cells (VPCs) (Eisenmann, 2005; Eisenmann et al., 1998). These six VPCs are competent to differentiate into one of two alternate vulval cell fates. (Though, P3.p, which is furthest away from the source of the WNT signal, adopts a VPC fate only in around 50% of the animals.) LIN-39 prevents the VPCs from fusing to the surrounding syncytial hypodermis (*hyp7*) by repressing, via the GATA transcription factors EGL-18 and ELT-6, the expression of the *eff-1* fusogen (Koh et al., 2002; Shemer and Podbilewicz, 2002, Fig. 1A). Moreover, the LIN-1 ETS and LIN-31 Forkhead transcription factors inhibit vulval differentiation by repressing the expression of *lin-39* and of the NOTCH ligand *lag-2* (Guerry et al., 2007; Wagmaister et al., 2006b; Zhang and Greenwald, 2011). Towards the end of the L2 stage, an inductive signal from the gonadal anchor cell (AC) selects the nearest VPC (P6.p) to adopt a primary (1°) vulval fate (Sternberg, 2005, Fig. 1B). The AC secretes the LIN-3 growth factor, which is homologous to the mammalian epidermal growth factor (EGF), and activates the EGF receptor homolog LET-23 in the VPCs. Downstream of LET-23, the canonical RAS/MAPK pathway controls the activity of transcription factors that specify the 1° cell fate (Sundaram, 2006). Activated MAPK phosphorylates the LIN-1 ETS and LIN-31 Forkhead transcription factors, which relieves their inhibitory effect on *lin-39* expression and permits vulval differentiation (Miller et al., 1993; Tan et al., 1998). Since the 1° VPC P6.p receives most of the inductive LIN-3 signal, it exhibits the highest LIN-39 expression (Malooof and Kenyon, 1998). LIN-39 plays essential roles during and after vulval fate specification. For example, during vulval fate specification LIN-39 induces the expression of the *lin-12 notch* receptor and its ligand *lag-2* (Regós et al., 2013; Takács-Vellai et al., 2007, Fig. 1B). Activation of the LIN-12 NOTCH receptor in P5.p and P7.p specifies the 2° and inhibits the 1° fate (Berset et al., 2001; Sundaram, 2006; Yoo et al., 2004). During the morphogenesis phase, LIN-39 promotes the proliferation of the vulval cells (Shemer and Podbilewicz, 2002) and activates the expression of *vab-23*, which is essential for the formation of the vulval toroids (Pellegrino et al., 2011).

One aspect of vulval development that is less understood is the control of VPC proliferation. The heterochronic genes *lin-14* and *lin-28* together with the MAPK targets *lin-31* and *lin-1* are required to arrest the VPCs during the L2 stage in the G1 phase of the cell cycle, in part by inducing the expression of the CDK inhibitor CKI-1 (Clayton et al., 2008; Hong et al., 1998; Hoyos et al., 1996; van den Heuvel, 2005, Fig. 1A). *lin-39*, on the other hand, is necessary for VPC proliferation after vulval induction, though the exact role of *lin-39* in cell cycle control has not been investigated (Shemer and Podbilewicz, 2002). Moreover, it is unclear if and how the activity of the EGFR and NOTCH signaling pathways coordinate cell cycle progression with vulval induction to maintain the proliferation of the differentiating vulval cells. Here, we show that the *hox* gene *lin-39* performs two distinct functions in order to link VPC fate specification and proliferation. First, LIN-39 maintains the VPCs competent to proliferate by directly inducing the expression of the core cell cycle regulators, such as *cye-1 cyclinE* and *cdk-4*. Second, LIN-39 activates the lateral NOTCH signaling pathway, which overcomes the LIN-31 mediated repression of the cell cycle.

2. Materials and methods

2.1. *C. elegans* methods and strains

All strains used were derived from the Bristol strain N2. Animals were cultivated under standard conditions at 20 °C as described in (Brenner, 1974) unless specified. The mutations used in

this study have been previously described and are listed below according to their linkage groups. To construct the different mutant combinations standard genetic methods were used.

Alleles used: LGII: *lin-31(n301)* (Miller et al., 1993), *cdc-14(he141)* (Saito et al., 2004), *lin-31(cp1)* (Dickinson et al., 2013), *eff-1(ok1021)* (Podbilewicz et al., 2006); LGIII: *lin-39(n1760)* (Clark et al., 1993); LGIV: *lin-3(e1417)* (Hwang and Sternberg, 2004), *lin-1(e1777)* (Ferguson and Horvitz, 1985).

Transgenes used: *mals113[Pcki-1::gfp, dpy-20(+)]* (Hong et al., 1998), *zhIs1[lin-39::gfp]* (Szabó et al., 2009), *zhIs038[let-23::gfp, unc-119(+)]* (Haag et al., 2014), *arIs82[lin-12::gfp; unc-4(+)]* (Shaye and Greenwald, 2002), *zhIs80[Pcye-1::gfp]*, *zhIs86[Pcye-1::gfp, unc-119(+)]*, *zhIs87[Pcye-1ΔHBS1::gfp, unc-119(+)]*, *zhIs88[Pcye-1ΔHBS2::gfp, unc-119(+)]*, *zhIs89[Pcye-1ΔHBS1ΔHBS2::gfp, unc-119(+)]*, *zhEx535[Pcdk-4::gfp]* (all this study), *zhEx500[Pbar-1::nicd::gfp, unc-119(+)]* (Nusser-Stein et al., 2012).

2.2. Plasmids and transgenic lines

Plasmid pDR8 (*Pcye-1::gfp*) was made by cloning the promoter and the first part of the coding region (−942 to +1375) in frame with the *gfp* cassette into the HindIII and Sall sites of plasmid pPD95.75 (gift from Andrew Fire, Stanford University School of Medicine). pDR10 (*Pcdk-4::gfp*) was made by introducing the *cdk-4* promoter region including the two annotated isoforms (−800 to +1588) into the BamHI and SphI sites of plasmid pPD96.04 (a gift from Andrew Fire). pDR11 (*Pcye-1::gfp, unc-119(+)*) was built by cloning a 4 kb *SpeI* fragment containing the *Pcye-1::gfp* reporter from the plasmid pDR8 into the *SpeI* site of the *mosSCI* vector pCFJ151 (Frøkjær-Jensen et al., 2008). pDR12 (*Pcye-1ΔHBS1::gfp, unc-119(+)*), pDR13 (*Pcye-1ΔHBS2::gfp, unc-119(+)*) and pDR15 (*Pcye-1ΔHBS1ΔHBS2::gfp, unc-119(+)*) were obtained by site-directed mutagenesis of the plasmid pDR11 introducing the mutations described in the results section. The primers used for plasmid constructions are listed in Table S1.

Worms carrying extra-chromosomal arrays were generated by microinjection of purified plasmids into the syncytial gonads of young adult worms (Mello et al., 1991). All constructs were injected at a concentration of 50 ng/μl. For *zhIs80* and *zhEx535* we used pCFJ90 (*Pmyo-2::mcherry*) as transformation marker at a concentration of 2.5 ng/μl (Frøkjær-Jensen et al., 2008). *zhIs80* was integrated through gamma irradiation to an unknown location in the genome. The total concentration of DNA was adjusted to 150 ng/μl by adding the plasmid pBluescript-KS. For the generation of the *mosSCI* lines (Frøkjær-Jensen et al., 2008), *zhIs86* to *zhIs89*, we injected the plasmids pDR11, pDR12, pDR13 or pDR15 together with the markers pCFJ90 (*Pmyo-2::mcherry*) at a concentration of 2.5 ng/μl, pCFJ104 (*Pmyo-3::mcherry*) at a concentration of 5 ng/μl and pGH8 (*Prap::mcherry*) at a concentration of 10 ng/μl, together with the *Mos1* transposase plasmid pJL43.1 at a concentration of 50 ng/μl.

2.3. Microscopy and image analysis

Animals were mounted on 4% agarose pads in 20 mM tetramisole hydrochloride in water. The vulval induction index was scored as described (Berset et al., 2001). To obtain synchronized late L2 larvae, oocytes were isolated by hypochlorite treatment of gravid adults, allowed to hatch in the absence of food for 24 h to obtain arrested L1 larvae that were transferred to plates containing OP50 bacteria and grown until they had reached the late L2/early L3 stage. For S-phase arrest, hydroxyurea was added to synchronized L2 larvae at a concentration of 40 mM as described (Ambros, 1999; Berset et al., 2001). The vulval invaginations and the number of cells per invagination were counted using Nomarski optics in a Leica DMRA microscope equipped with a CCD camera

(Hamamatsu ORCA-ER) controlled by the Openlab 5 software (Improvision). To quantify GFP reporter expression, a calibrated fluorescent light source (X-Cite exacte, Excelitas Technologies Corp) was used on the same microscope. To compare GFP intensities in the *eff-1(lf)* and *eff-1(lf); lin-39(lf)* backgrounds, images were acquired under the same illumination conditions and acquisition settings. Fluorescent signal intensities in the VPC nuclei were quantified using the Fiji software as described (Nusser-Stein et al., 2012; Schindelin et al., 2012).

2.4. ChIP-Q-PCR analysis

Chromatin extracts were prepared from 100 ml mixed-stage liquid cultures of animals carrying the *zhls1[lin-39::gfp]* and *zhls89[Pcye-1ΔHBS1ΔHBS2::gfp]* arrays as described (Pellegrino et al., 2011). As negative controls, extract from animals carrying only *zhls89[Pcye-1ΔHBS1ΔHBS2::gfp]* were prepared and processed in parallel. Cross-linking was done with 1% paraformaldehyde for 20 min at room temperature. LIN-39::GFP bound chromatin was precipitated using GFP-Trap[®] antibodies (Chromotek) as described by Pellegrino et al. (2011) with the following modification: Extracts were pre-cleared by incubation with Dynabeads (10 μl per sample) before adding GFP-Trap[®] beads (20 μl per 4–5 mg of total protein in the extracts). After reverse cross-linking, binding of LIN-39::GFP to the different sites was quantified by Q-PCR using an ABI Prism 7900HT thermocycler with the MESA Green mastermix plus (Eurogentec) and primers specific for the wild-type HBS in endogenous *cye-1* and the mutant HBS in the *zhls89* reporter (for the sequences of the primer used see Table S1). For each measurement, the signal was first normalized to the signal obtained from the input DNA (% input). To calculate the specific enrichment, the % input value obtained from the *zhls1[lin-39::gfp]; zhls89[Pcye-1ΔHBS1ΔHBS2::gfp]* strain was divided by the % input value obtained from the *zhls89[Pcye-1ΔHBS1ΔHBS2::gfp]* negative control strain. In addition to the Q-PCR assays in the HBS regions, we used a primer pair in the 3' UTR of *cye-1* and a primer pair spanning the *cye-1::gfp* fusion in the *zhls89* reporter, respectively. The data in Fig. 3H show the average ratios obtained in three independent experiments.

2.5. Statistical analysis

t-tests for independent samples were used to determine the statistical significance of differences. Where specified the Fisher's exact probability test was performed. In all figures, * indicates $p < 0.05$, ** $p < 0.005$ and *** $p < 0.001$. Statistical analysis of the *cye-1::gfp* expression intensities is shown in Table S2.

3. Results

3.1. The VPCs in *lin-39* mutants are partially sensitive to the inductive LIN-3 signal but they do not proliferate

Shemer et al. (Shemer and Podbilewicz, 2002) originally reported that in *lin-39(lf)* mutants carrying in addition a loss-of-function (*lf*) mutation in *eff-1* to prevent the fusion of the Pn.p cells with the hypodermis, the Pn.p cells remained as polarized epithelial cells, but they failed to proliferate. Despite the loss of Pn.p cell proliferation, the proximal cells P5.p, P6.p and P7.p occasionally formed a vulval invagination containing three to four cells, indicating that Pn.p cells lacking *lin-39* can differentiate as long as they are maintained as polarized epithelial cells. These observations indicated that *lin-39* plays a pivotal role as a regulator of cell cycle in the VPCs (Shemer and Podbilewicz, 2002).

Building on these findings, we first investigated the capability

of the Pn.p cells in *eff-1(lf); lin-39(lf)* double mutants to receive the inductive LIN-3 EGF or lateral LIN-12 NOTCH signal. A functional reporter for the *let-23* *egf* receptor (Haag et al., 2014) was expressed in P6.p in around 20% of *eff-1(lf); lin-39(lf)* double mutants ($n=22$) as opposed to 80% of *eff-1(lf)* single mutants ($n=20$), which we used as control strain throughout this study (Fig. 1C,C'). By contrast, the expression of a LIN-12::GFP reporter (Shaye and Greenwald, 2002), which was localized on the apical surface of the VPCs in all *eff-1(lf)* animals examined, was not detectable in *eff-1(lf); lin-39(lf)* double mutants (Fig. 1D,D') ($n=20$ for each genotype). Thus, the Pn.p cells in *lin-39(lf)* mutants may remain partially competent to receive the inductive AC signal.

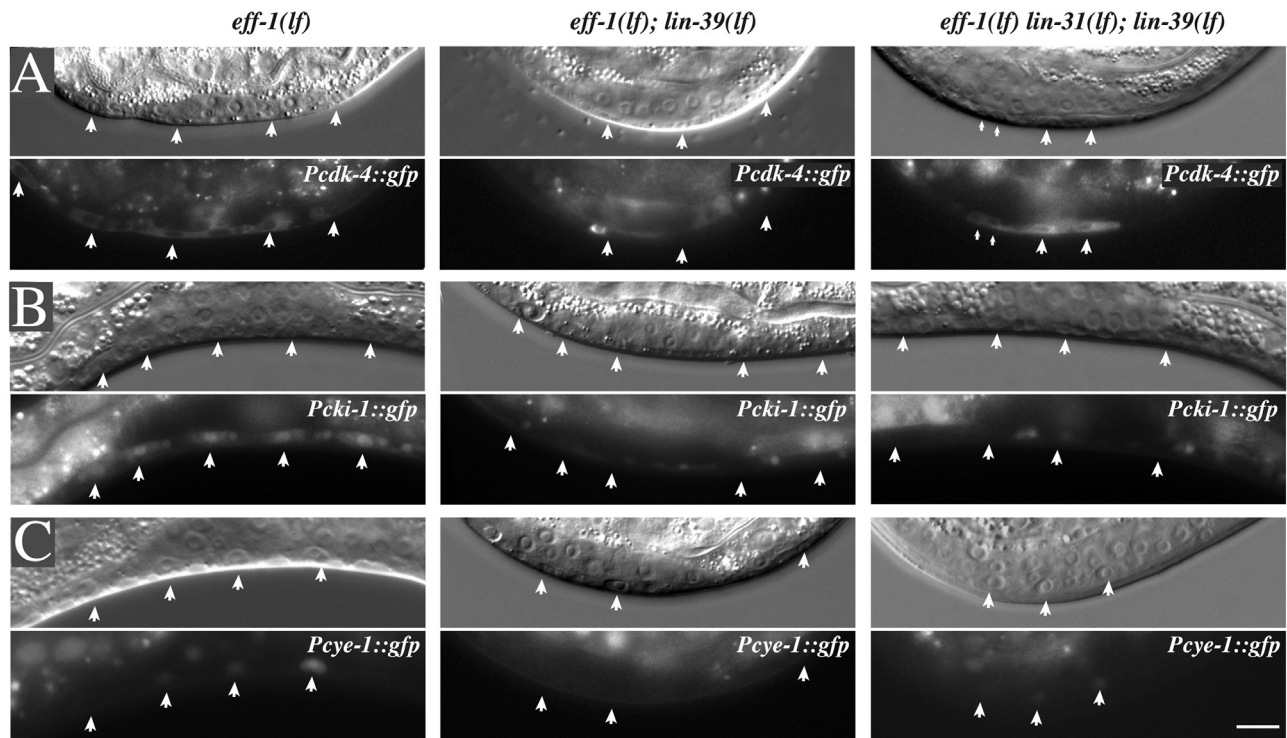
We observed a vulval invagination in the mid-body region underneath the AC in 11% of *eff-1(lf); lin-39(lf)* double mutants (Fig. 1E and Table S3). While the invaginations of *eff-1(lf)* single mutants always contained 22 differentiated vulval cells as in wild-type larvae, the invaginations in the *eff-1(lf); lin-39(lf)* double mutants on average contained 3.8 cells, as these invaginations were mostly formed by three undivided Pn.p cells (Fig. 1F and Table S3). To test if the inductive LIN-3 EGF signal plays a role in inducing vulval differentiation in the absence of LIN-39, we introduced the *lin-3(e1417)* allele, which specifically reduces *lin-3* *egf* expression in the AC (Hwang and Sternberg, 2004), into the *eff-1(lf); lin-39(lf)* background. Even though the *lin-3(e1417)* allele does not completely block vulval induction (Table S3), none of the *eff-1(lf); lin-39(lf); lin-3(lf)* triple mutants examined developed a vulval invagination (Fig. 1C,D and Table S3).

We conclude that those Pn.p cells, which formed a vulval invagination in *eff-1(lf); lin-39(lf)* double mutants (11% of the cases), had responded to the inductive LIN-3 EGF signal, but they did not proliferate. Thus, *lin-39* is essential to promote VPC proliferation even though Pn.p cells lacking *lin-39* remain partially sensitive to the inductive LIN-3 EGF signal.

3.2. *lin-39* induces the expression of the cell cycle regulators *cye-1*, *cki-1* and *cdk-4*

To characterize the role of LIN-39 in regulating VPC proliferation, we explored the modENOCODE data (Niu et al., 2011) and searched for predicted LIN-39 binding sites in the 5' regulatory regions or in introns of genes encoding known cell cycle regulators. We found predicted LIN-39 binding sites in at least 17 regulators of the cell cycle; these are *cki-1*, *cdk-4*, *cye-1*, *cdc-14*, *cdk-1*, *cdk-7*, *lin-35*, *efl-1*, *lin-9*, *mat-1*, *mrt-2*, *cul-1*, *san-1*, *mdf-1*, *wee-1.3*, *lin-23* and *lin-36* (van den Heuvel, 2005). We focussed on regulators of the G1 to S-phase transition because the VPCs arrest in the G1 phase during the L2 stage and progress into the S phase after adopting their fates at the late L2/ early L3 stage. We observed strong LIN-39 binding sites in the genes encoding the CDK kinase CDK-4 (Park and Krause, 1999) and in the G1/S phase cyclin CYE-1 (Gleason et al., 2000, Fig. S1 and Fig. 3A). Weaker binding sites were also observed in the *cki-1* locus, which encodes a CDK inhibitor of the p21 family (Hong et al., 1998, Fig. S1).

To investigate whether *lin-39* controls the expression of these G1/S-phase regulators in the VPCs, we compared the expression patterns of transcriptional *gfp* reporters in *eff-1(lf)* single versus *eff-1(lf); lin-39(lf)* double mutants that were synchronized at the mid to late L2 stage, shortly before the VPCs normally begin to proliferate (see Section 2). For *cdk-4*, we constructed a reporter that includes the two alternative first exons and 1 kb of 5' regulatory sequences containing the predicted LIN-39 binding site and all the previously identified regulatory elements (Brodigan et al., 2003). The frequency of VPCs expressing *Pcdk-4::gfp* was reduced from nearly 50% in *eff-1(lf)* single mutants to less than 10% in *eff-1(lf); lin-39(lf)* double mutants (Fig. 2A,D). Similarly, the expression of a *Pcki-1::gfp* reporter containing 8 kb of 5' regulatory



D

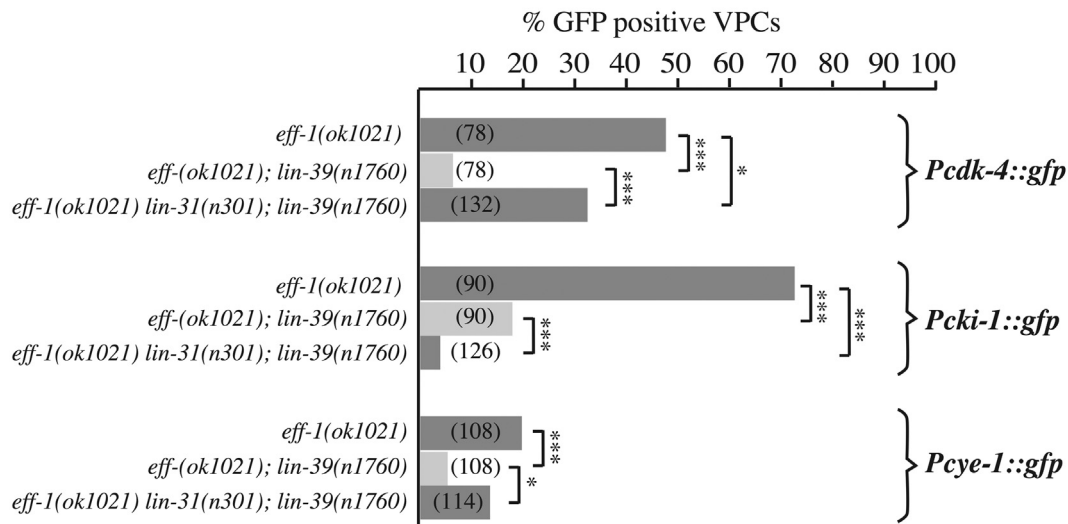


Fig. 2. Reduced *cdk-4*, *cki-1* and *cy-1* reporter expression in *lin-39* mutants and re-activation in *lin-31* mutants. (A) Expression of the transcriptional *Pcdk-4::gfp*, (B) *Pcki-1::gfp* and (C) *Pcy-1::gfp* reporters. The first rows show the Nomarski images of (from left to right) *eff-1(ok1021)* single, *eff-1(ok1021); lin-39(n1760)* double and *lin-31(n301) eff-1(ok1021); lin-39(n1760)* triple mutants. *Pcdk-4::gfp* and *Pcki-1::gfp* were analyzed in mid L2 larvae (26 h after L1 arrest); *Pcy-1::gfp* expression was scored in S-phase arrested early L3 larvae by exposing mid L2 larvae (26 h after L1 arrest) for 4 h to 40 mM hydroxyurea (see Section 2). The arrowheads point at the positions of the VPC nuclei and the two smaller arrows in the right panel of (A) indicate duplicated VPCs. The scale bar in (C) is 10 μ m. (D) Percentage of VPCs expressing the cell cycle reporters in the different genetic backgrounds shown in (A) through (C). The number of VPCs analyzed for each genotype is shown in brackets. Statistical significance was analyzed with a Fisher's exact probability test; * signifies $p < 0.05$ and *** $p < 0.001$.

sequences and the endogenous 3' UTR (Hong et al., 1998) was reduced from around 70% GFP positive VPCs in single to fewer than 20% in *eff-1(lf); lin-39(lf)* double mutants (Fig. 2B,D). To analyze *cy-1* expression, we generated a *Pcy-1::gfp* reporter (*zhIs80*), in which a *gfp* cassette was fused in frame into the third exon, such that both predicted LIN-39 binding sites were included as well as the previously described domains that are necessary for *cy-1* expression (Brodigan et al., 2003, Fig. 3A). Since the *Pcy-1::gfp* reporter is only transiently expressed in the VPCs at the late

G1/early S-phase, we exposed late L2 larvae for four hours to hydroxyurea (HU) to arrest their cell cycle in the early S-phase before analyzing *Pcy-1::gfp* expression (see Section 2). With this procedure we were able to detect *cy-1::gfp* expression in around 20% of the VPCs in *eff-1(lf)* single mutants (Fig. 2C,D). Similar to the other cell cycle regulators, *Pcy-1::gfp* expression was strongly reduced in *eff-1(lf); lin-39(lf)* double mutants.

In summary, the transcriptional reporter analysis indicated that *lin-39* is necessary for the expression of *cdk-4*, *cki-1* and *cy-1* in

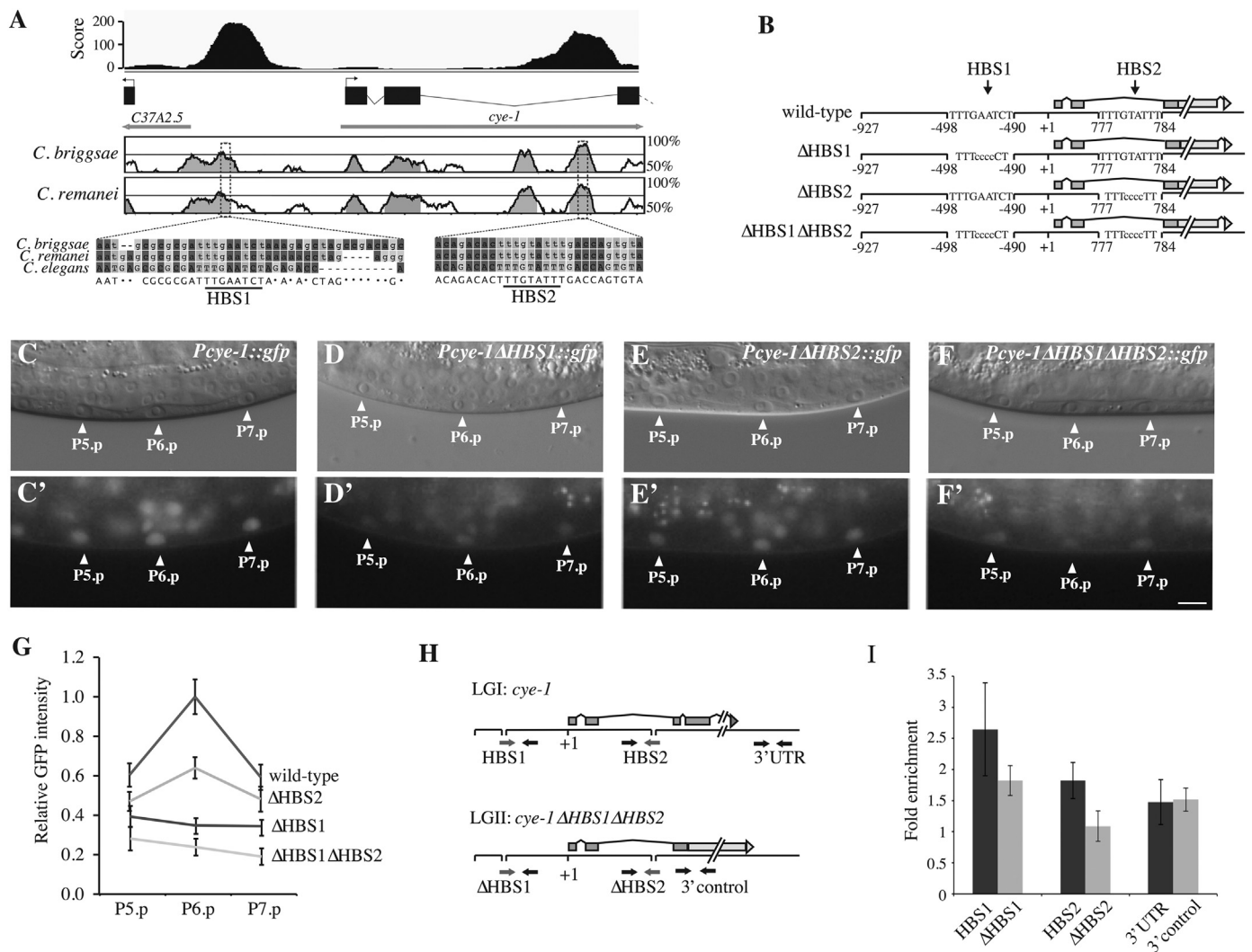


Fig. 3. LIN-39 regulates *cye-1* expression via conserved HBS motifs. (A) The top graph shows the LIN-39 ChIP read counts in the *cye-1* genomic region as reported by modENCODE (Niu et al., 2011). The sequence conservation between the *C. elegans*, *C. briggsae* and *C. remanei* *cye-1* loci is shown in the graphs underneath with the sequence alignments of the two LIN-39 binding sites containing conserved HBS motifs. (B) Structure of the wild-type *cye-1* reporter and the Δ HBS1 and Δ HBS2 single and double mutants (the mutations in the two HBS motifs). (C–F) Expression pattern of the wild-type *cy-1::gfp* reporter and the Δ HBS1 and Δ HBS2 single and double mutants in the VPCs of early L3 larvae. The arrowheads point at the positions of the VPC nuclei, and the scale bar in (F') is 10 μ m. (G) Quantification of wild-type and mutant *cy-1::gfp* reporter expression in P5.p through P7.p in early L3 larvae. All values were normalized to the average GFP intensity measured with the wild-type reporter in P6.p. A statistical analysis of the data is shown in supplementary Table S1. (H) Location of the PCR primers used for ChIP-Q-PCR analysis of endogenous *cy-1* on LGI and the *cy-1 Δ HBS1 Δ HBS2* reporter on LGII. Grey primers indicate genotype specific binding. (I) Enrichment of LIN-39::GFP at the HBS sites of endogenous *cy-1* (dark grey columns) and the Δ HBS1 Δ HBS2 reporter (light grey columns). The specific enrichment was calculated as described in Section 2, and the average values obtained in three independent experiments are shown. The error bars represent the standard error of the mean (s.e.m.).

the VPCs of L2 larvae. Since the modENCODE project detected LIN-39 binding sites in several additional -positive and negative- cell cycle regulators, LIN-39 may act as a permissive factor that maintains the expression of the cell cycle machinery.

3.3. LIN-39 induces *cy-1* expression through a non-canonical HOX Binding Site

Even though the modENCODE data indicated the presence of LIN-39 HOX binding sites (HBS) in several cell cycle regulators, we could not identify the canonical HOX/PBX consensus motif TGATNNAT (Mann and Affolter, 1998) within the predicted binding regions. However, by searching for a common motive within the LIN-39 binding regions of cell cycle regulators and by filtering them using the syntenic regions in the *Caenorhabditis briggsae* and *Caenorhabditis remanei* genomes, we identified conserved sequence blocks containing the motif TTTG(A/T)AT(T/C)T, which appears to be diverged from the canonical HOX/PBX binding motif

TGATNNAT (Fig. 3A and Fig. S1).

To test if LIN-39 directly activates *cy-1* expression through these non-canonical HBSs, we generated four variants of the *cy-1::gfp* reporter and integrated single copies of each reporter at a defined location on chromosome II using the *mosSCI* technique (Frøkjær-Jensen et al., 2008): a wild-type reporter with both HBSs intact (*zhls86*); the Δ HBS1 reporter (*zhls87*), in which the HBS upstream of the promoter had been mutated from TTTGAATCT to TTTCCCCCT, the Δ HBS2 reporter (*zhls88*), in which the HBS in the second intron had been mutated from TTTGTATTT to TTTCCCCCT, and the Δ HBS1 Δ HBS2 reporter (*zhls89*), in which both HBSs had been mutated (Fig. 3B). We then measured for each reporter the relative *cy-1::gfp* signal intensity in the VPCs of early L3 larvae. Expression of the wild-type reporter was robust and significantly stronger in the 1° VPCs than in the 2° VPCs (Fig. 3C,G and Table S2 for statistical analysis). The Δ HBS1 reporter showed overall reduced and equal expression levels in the 1° and 2° VPCs (Fig. 3D, G). By contrast, the Δ HBS2 reporter exhibited only a slight

reduction in the expression levels and maintained the bias towards 1°-specific expression (Fig. 3E,G). Finally, the expression of the Δ HBS1 Δ HBS2 reporter was further reduced when compared to either single mutant Δ HBS reporter (Fig. 3F,G). Thus, the two HBS cooperatively induce *cye-1* expression in the VPCs. Though, the HBS1 site seems to introduce a 1° lineage-specific bias and overall contributes to a greater extent than the HBS2 site. This 1°-lineage bias could be due to the higher *lin-39* levels in the 1° VPC (Maloor and Kenyon, 1998).

To confirm the binding of LIN-39 to the HBS motifs in *cye-1*, we performed chromatin immunoprecipitation (ChIP) experiments combined with quantitative real-time PCR (Q-PCR) analysis as described previously (Pellegrino et al., 2011, see also Section 2). By using chromatin extracts of mixed-stage transgenic animals carrying a single copy of the Δ HBS1 Δ HBS2 reporter integrated on chromosome II and a functional *lin-39::gfp* transgene, we could directly compare LIN-39 binding to the wild-type (endogenous) and the mutant (transgenic) HBS motifs in the same chromatin preparation. For this purpose, we designed PCR primer pairs specifically amplifying either of the two wild-type HBSs in endogenous *cye-1* on chromosome I or the mutant HBSs in the Δ HBS1 Δ HBS2 reporter on chromosome II (Fig. 3H).

Q-PCR analysis of LIN-39::GFP ChIP revealed a nearly two-fold enrichment of LIN-39 binding at the wild-type HBS1 site in the endogenous *cye-1* locus compared to the ChIP from control animals lacking the *lin-39::gfp* transgene, confirming the specific LIN-39 binding to the wild-type HBS1 (Fig. 3I shows the average values of three completely independent experiment). On the other hand, LIN-39 was only slightly enriched (around 1.2 fold) at the mutant Δ HBS1 in the *cye-1* reporter on chromosome II. Despite the clear LIN-39 peak observed by modENCODE at the HBS2 in the second intron of *cye-1*, we detected only a very slight enrichment of LIN-39::GFP at this site when compared to negative control ChIP lacking LIN-39::GFP (Fig. 3I). This may be due to a much weaker or more transient binding of LIN-39 to the HBS2 motif.

Taken together, the results of the ChIP analysis are consistent with the relatively mild effect of the Δ HBS2 mutation on *Pcye-1::gfp* expression and support the conclusion that the HBS1 site is the main LIN-39 response element in *cye-1*. Given the sequence conservation in the LIN-39 binding sites in the *cki-1* and *cdk-4* genes detected by modENCODE, it seems likely that LIN-39 also binds to the HBS motifs in other cell cycle regulator genes.

3.4. The *lin-31* forkhead transcription factor inhibits Pn.p cell proliferation

Since LIN-39 is expressed in the VPCs immediately after they are born at the late L1 stage (Clark et al., 1993; Wagmaister et al., 2006a), we hypothesized that additional factors should exist to counteract LIN-39 activity and block proliferation until the vulval cell fates have been specified towards the end of the L2 stage. A complex of the LIN-1 ETS and LIN-31 Forkhead transcription factors plays an important role in inhibiting vulval differentiation and maintaining VPC quiescence (Jacobs et al., 1998; Tan et al., 1998). In particular, LIN-1 and LIN-31 repress the transcription of *lin-39* and promote the expression of *cki-1* (Clayton et al., 2008; Guerry et al., 2007; Wagmaister et al., 2006b). To test if LIN-31 or LIN-1 repress VPC proliferation in addition to inhibiting *lin-39* and promoting *cki-1* expression, we examined Pn.p cell proliferation in *eff-1(lf) lin-31(lf); lin-39(lf)* and *eff-1(lf); lin-39(lf); lin-1(lf)* triple mutants (Fig. 4A). To quantify proliferation, we counted the frequency of animals developing at least one invagination at the L4 stage (Fig. 4B), as well as the average number of differentiated cells per invagination among the animals with invaginations (Fig. 4C). Due to the variable position of the Pn.p cells and their descendants in *eff-1(lf); lin-39(lf)* double mutants, it was impossible to

unambiguously identify the individual cell lineages. Therefore, supplementary Table S3 shows the relative positions of the invaginations in the different genotypes, which we scored by defining 6 zones along the anterior-posterior axis as described in the table legend.

The *lin-31(lf)* but not the *lin-1(lf)* mutation rescued the proliferation defect of *eff-1(lf); lin-39(lf)* animals (Fig. 4A). In *eff-1(lf) lin-31(lf); lin-39(lf)* triple mutants, we observed an increase in the frequency of Pn.p cells forming an invagination (Fig. 4B) as well as in the number of differentiated cells per invagination (Fig. 4C). In contrast to *lin-31(lf)*, the *lin-1(lf)* mutation did not increase the frequency of invaginations or the number of cells per invagination in the *eff-1(lf); lin-39(lf)* background (Fig. 4 and Table S3). Moreover, we did not observe an additional increase in the frequency of invaginations in *eff-1(lf) lin-31(lf); lin-39(lf); lin-1(lf)* quadruple mutants, and the average number of cells per invagination was not significantly increased compared to *eff-1(lf) lin-31(lf); lin-39(lf)* triple mutants (Fig. 4B,C and Table S3).

While the invaginations in *eff-1(lf); lin-39(lf)* double mutants always formed in the mid body region underneath the AC, the invaginations in *eff-1(lf) lin-31(lf); lin-39(lf)* and *eff-1(lf); lin-39(lf); lin-1(lf)* triple mutants were frequently shifted towards the posterior body region, suggesting an AC-independent induction of vulval differentiation (Fig. 4A and Table S3). Moreover, the *lin-31(lf)* mutation not only caused Pn.p cell proliferation in the absence of *lin-39*, but it also re-activated the expression of the cell cycle reporters. Especially, the frequency of Pn.p cells expressing *cye-1::gfp* and *cdk-4::gfp* was significantly increased in *eff-1(lf) lin-31(lf); lin-39(lf)* triple compared to and *eff-1(lf); lin-39(lf)* double mutants (Fig. 2A,C,D). On the other hand, the expression of *cki-1::gfp* was not restored by the *lin-31(lf)* mutation (Fig. 2B,D) because LIN-31 positively regulates *cki-1* expression (Clayton et al., 2008). We therefore tested if a loss-of-function mutation in the CKI-1 activator *cdc-14* (Roy et al., 2011; Saito et al., 2004) was sufficient to rescue the Pn.p proliferation defect of *eff-1(lf); lin-39(lf)* mutants. However, the inactivation of CKI-1 through a *cdc-14(lf)* mutation did not induce Pn.p cell proliferation in the *eff-1(lf); lin-39(lf)* background (Table S3 and data not shown).

Taken together, these results indicate that LIN-31 inhibits cell cycle progression independently of LIN-39 and LIN-1. For this purpose, LIN-31 induces *cki-1* and represses *cdk-4* and *cye-1* expression to arrest the VPCs in the G1 phase. During vulval induction, phosphorylation of LIN-31 by the MAPK likely inactivates this repressor function of LIN-31 and releases the inhibition of the VPC cycle (Tan et al., 1998).

3.5. LIN-12 NOTCH signaling promotes VPC proliferation in parallel with LIN-31

Neither *lin-12 notch* nor its ligand *lag-2 delta* are expressed in the VPCs of *lin-39(lf)* mutants (Fig. 1D and Regős et al., 2013; Zhang and Greenwald, 2011). We thus tested if the VPC proliferation defect of *eff-1(lf); lin-39(lf)* double mutants could be rescued by forced activation of the NOTCH signaling pathway. For this purpose, we introduced a transgene expressing the intracellular LIN-12 domain (NICD) under the control of the *bar-1* promoter, which is active in all VPCs (*Pbar-1::nicd::gfp*) (Nusser-Stein et al., 2012). In the *eff-1(lf)* background, the *Pbar-1::nicd::gfp* transgene caused ectopic 2° fate specification in all VPCs except for P6.p, which was induced by the AC signal to adopt a 1° fate. Similar to the *lin-31(lf)* mutation, the *Pbar-1::nicd::gfp* transgene restored VPC proliferation and caused the formation of ectopic vulval invaginations in the *eff-1(lf); lin-39(lf)* background (Fig. 4 and Table S3). Furthermore, we observed a similar shift of the vulval invaginations towards the posterior body region as described above for the *lin-31(lf)* mutation (Fig. 4A and Table S3).

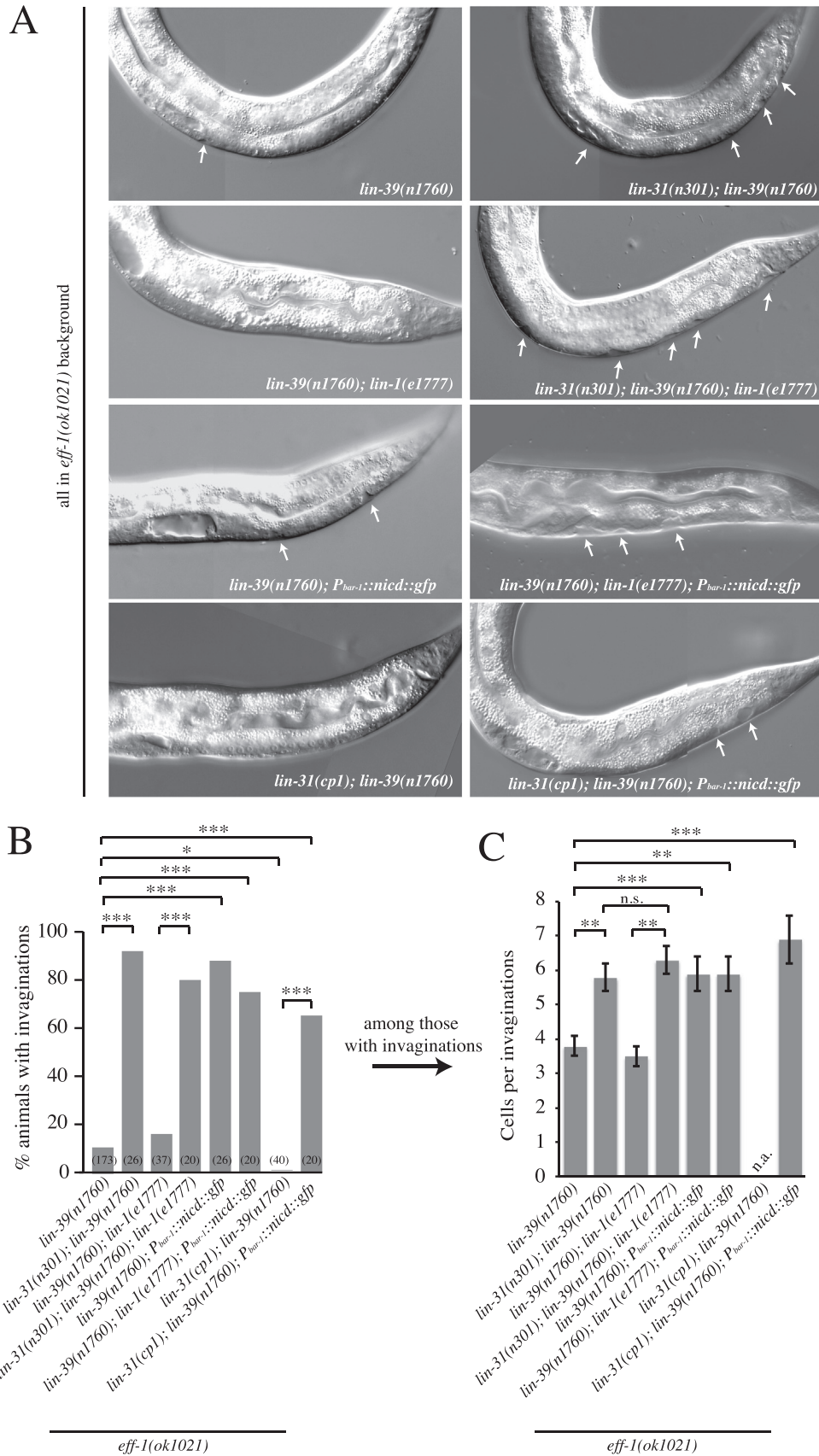


Fig. 4. Suppression of the *lin-39* proliferation defect by *lin-31(lf)* or by NOTCH signaling. (A) Nomarski image of representative animals for each genotype are shown. Arrows indicate the position of the invaginations. (B) Percentage of animals with invaginations at the L4 stage. Numbers in brackets indicate the number of animals analyzed for each genotype. (C) Average number of cells per invagination in those animals developing at least one invagination. Error bars indicate the standard error of the mean (s.e.m.). Statistical significance was analyzed with a T-test; * signifies $p < 0.05$, **signifies $p < 0.005$ and *** $p < 0.001$.

We have previously reported that the non-phosphorylated form of LIN-1 is required for certain aspects of 2° cell fate execution acting downstream of the NOTCH pathway, indicating a dual function of LIN-1 depending on its phosphorylation status (Farooqui et al., 2012). We therefore tested if LIN-1 also acts downstream of the NOTCH pathway to promote the cell cycle progression. To this aim, we crossed the *lin-1(lf)* allele *e1777* into the *eff-1(lf); lin-39(lf); P_{bar-1::nicd::gfp}* strain (Fig. 4A). *lin-1(lf)* did not significantly suppress the Pn.p cell proliferation induced by the *P_{bar-1::nicd::gfp}* transgene (Fig. 4B,C and Table S3). Thus, the activation of NOTCH signaling promotes VPC proliferation independently of LIN-1.

One possible scenario is that NOTCH signaling activates VPC proliferation by inactivating LIN-31, for example by inducing LIN-31 phosphorylation. Alternatively, NOTCH signaling may bypass the LIN-31-mediated repression of the cell cycle and induce VPC proliferation independently of LIN-31. To distinguish between these two scenarios, we examined the epistatic interaction between *lin-12 notch(gf)* and the constitutively active, phosphorylation-deficient *lin-31(cp1)* mutant, in which the four threonine residues that are phosphorylated by the MAPK (T145, T200, T218 and T220) had been mutated into alanine (Dickinson et al., 2013). *lin-31(cp1)* completely suppressed the residual proliferation occurring in *eff-1(lf); lin-39(lf)* double mutants, as none of the *eff-1(lf) lin-31(cp1); lin-39(lf)* triple mutants examined developed a vulval invagination (Fig. 4 and Table S3). Thus, *lin-31(cp1)* acts as a repressor of VPC proliferation. If the NOTCH pathway activates VPC proliferation by inactivating LIN-31, then the *lin-31(cp1)* mutation should suppress VPC proliferation in *eff-1(lf); lin-39(lf); P_{bar-1::nicd::gfp}* animals. However, the *lin-31(cp1)* allele had no effect on VPC proliferation in the *eff-1(lf); lin-39(lf) P_{bar-1::nicd::gfp}* background, as neither the frequency of invaginations nor the number

of cells per invagination were significantly reduced (Fig. 4 and Table S3).

Taken together, the epistasis analysis indicates that NOTCH signaling promotes VPC proliferation independently of LIN-1 and of LIN-31 phosphorylation. We conclude that NOTCH signaling induces VPC proliferation via a separate pathway acting in parallel with LIN-1 and LIN-31.

4. Discussion

hox genes encode homeodomain transcription factors that control cell proliferation in a variety of tissues in different organisms (Hombria and Lovegrove, 2003; Rezsóhazy et al., 2015). Known examples include cell proliferation during insect and vertebrate limb development (Cohn et al., 1997; Mahfooz et al., 2004), tail regeneration in the zebrafish (Thummel et al., 2007) or hematopoietic stem cell expansion (Schiedlmeier et al., 2007). Moreover, de-regulated *hox* gene expression caused by chromosomal translocations or other mutations has been observed in different types of leukemia (Schiedlmeier et al., 2007). In most of these cases the HOX proteins were found to control proliferation indirectly by inducing secondary target genes that act as cell fate determinants or signaling molecules, which in turn control proliferation (Rezsóhazy et al., 2015).

By contrast, our data on *C. elegans* vulval development indicate that the *hox* gene *lin-39* actively promotes cell cycle progression by directly inducing the expression of core cell cycle regulators. LIN-39 binds to a conserved sequence motif in the G1 cyclin gene *cye-1* and possibly also in other genes encoding regulators of the G1 to S-phase transition such as *cdk-4* and *cki-1*. Interestingly, the LIN-39 binding sites in these genes contain a non-canonical motif that

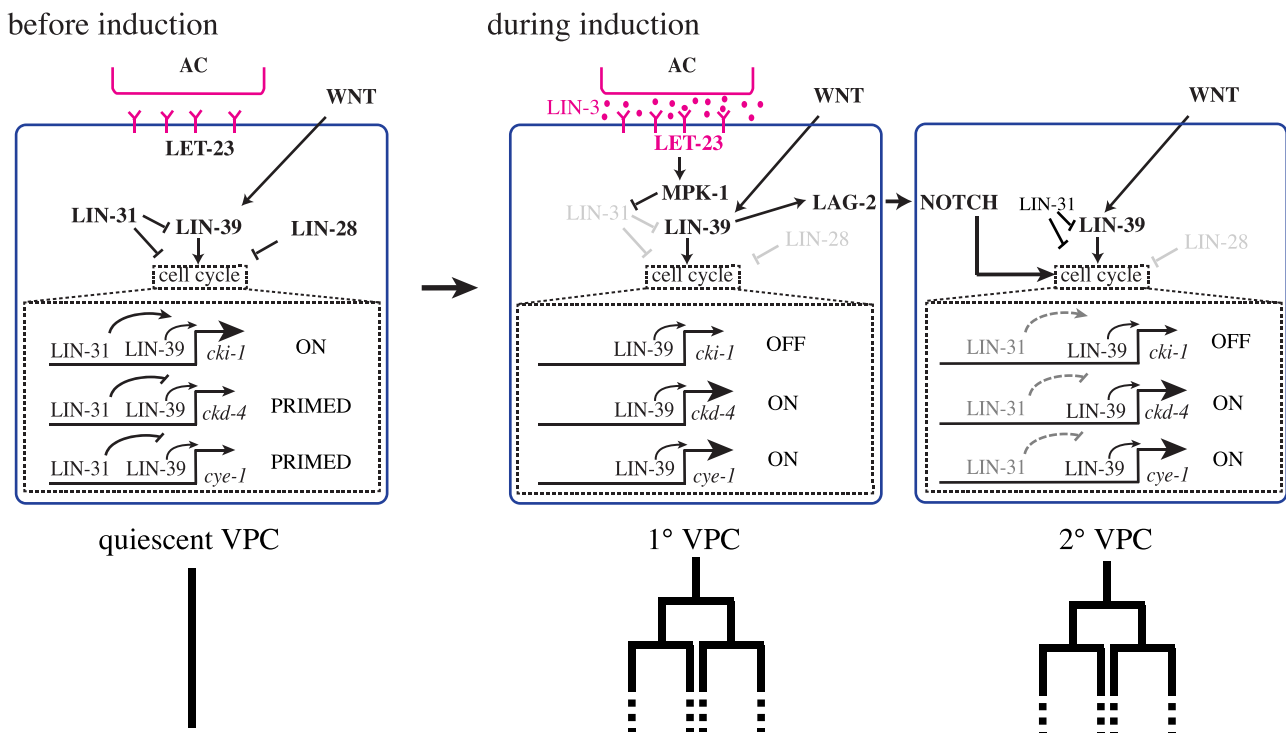


Fig. 5. Model for the regulation of VPC proliferation. Left cell: Before vulval induction, LIN-1 and LIN-31 repress *lin-39* expression, while WNT signaling induces LIN-39 expression in all VPCs. LIN-39 maintains basal expression of the cell cycle regulators *cye-1* and *cdk-4* to prime the VPCs for later proliferation. In addition, LIN-31 promotes *cki-1* and represses *cye-1* and *cdk-4* expression, thereby inducing VPC quiescence. Middle cell: During vulval induction, EGFR/RAS/MAPK signaling in the 1° VPC results in the inactivation of the LIN-1/LIN-31 complex via MAPK phosphorylation and hence a de-repression of *lin-39*. High LIN-39 levels induce *cye-1*, *cdk-4* and *lag-2* expression, while *cki-1* levels decline due to the inactivation of LIN-31. LAG-2 from the 1° VPC activates lateral NOTCH signaling in the adjacent 2° VPCs P5.p and P7.p. Right cell: NOTCH signaling in the 2° VPCs P5.p and P7.p overcomes the LIN-31 repressor activity. Thus, the inactivation of LIN-1/LIN-31 by RAS/MAPK signaling in the 1° VPC and the activation of NOTCH signaling in P5.p & P7.p lead to cell cycle progression upon vulval induction.

appears to be derived from the canonical HOX/PBX binding site (Mann and Affolter, 1998). The choice of HOX binding sites may be determined by the type of co-factor present in the specific cellular context. The two known HOX co-factors in *C. elegans*, CEH-20 PBX and UNC-62 MEIS have so far not been implicated in controlling VPC proliferation (Yang et al., 2005). Moreover, the existing ChIP-seq data do not indicate a clear enrichment of UNC-62 at the HBSS in the *cye-1* and *cdk-4* genes (Niu et al., 2011) (and own observation). On the other hand CEH-20 PBX negatively regulates *eff-1* expression in the VPCs (Shemer and Podbilewicz, 2002) and may therefore also act as a LIN-39 cofactor to control VPC proliferation.

By integrating our data into the existing framework of vulval differentiation (Fig. 1A), we propose the following model explaining how *lin-39* *hox* coordinates VPC cell fate specification with proliferation (Fig. 5). When the Pn.p cells are born at the end of the L1 stage, a WNT signal produced by tail cells induces basal levels of *lin-39* expression to block cell fusion and specify the VPC fate in the Pn.p cells of the mid-body region (P3.p through P8.p). At the same time, LIN-39 maintains the expression of core cell cycle regulators such as *cdk-4* and *cye-1*, keeping the VPCs competent to divide at a later stage (Fig. 5, left cell). Interestingly, LIN-39 also activates the transcription of the cell cycle inhibitor *cki-1*. This observation may initially appear contradictory to the role of LIN-39 in promoting VPC proliferation. However, the relationship between positive and negative cell cycle regulators is complex. The mammalian CDK-4/Cyclin D complex sequesters the CKI-1 homolog p27/KIP1, which in turn stabilizes the CDK-4/Cyclin D complex (Cheng et al., 1999). Thus, LIN-39 may activate the entire cell cycle machinery rather than individual components to ensure a regulated G1/S phase transition of the VPCs upon vulval induction.

In addition, the heterochronic protein LIN-28 and the LIN-31 transcription factor arrest the VPC cycle in the G1 phase by activating the expression of *cki-1* and, at least in the case of LIN-31, by repressing *cdk-4* and *cye-1* expression. As a result of these interactions, the VPCs remain in the G1 phase until the end of the L2 stage, when LIN-28 levels are declining. At this stage, the 1° and 2° fates are specified by the inductive EGFR and the lateral NOTCH signals (Fig. 5, middle and right cells). EGFR/RAS/MAPK signaling in the 1° lineage causes the phosphorylation and inactivation of LIN-31 and LIN-1, which results in reduced *cki-1* and increased *lin-39*, *cdk-4* and *cye-1* levels (Malooof and Kenyon, 1998; Tan et al., 1998). Activation of the NOTCH pathway in the 2° VPCs by the lateral signal from the 1° VPC promotes cell cycle progression independently of LIN-39, LIN-1 and LIN-31. Since lateral NOTCH signaling efficiently blocks EGFR/RAS/MAPK signaling in the 2° lineage (Berset et al., 2001; Yoo et al., 2004), NOTCH probably promotes cell cycle progression in a MAPK-independent fashion. Whether NOTCH signaling directly up-regulates the expression of cell cycle regulator genes in the 2° lineage or if NOTCH overcomes the LIN-31 repressor activity through another mechanism remains to be determined. However, since the forced expression of NICD did not completely rescue the *lin-39(lf)* proliferation defect, LIN-39 and NOTCH signaling are likely to act in parallel.

In summary, we have found that the HOX protein LIN-39 regulates the VPC cycle at two levels. First, LIN-39 acts as a permissive factor by maintaining the expression of the cell cycle machinery in the VPCs, keeping them competent to proliferate. Second, LIN-39 triggers the lateral NOTCH signaling pathway in the adjacent 2° VPCs, which overcomes the cell cycle inhibition by LIN-31 Forkhead. LIN-39 is therefore a central node in a network that coordinates VPC proliferation with fate specification.

Acknowledgments

We wish to thank all past and present members of the Hajnal

lab for their inputs and comments throughout this work. We are grateful to Erika Fröhli for her technical support. We are also grateful to the Saito and Kim labs for sharing reagents and to the *C. elegans* genetics center for providing strains. This work was supported by a grant from the Swiss National Science Foundation no. 31003A_146131 to A.H. and the Kanton Zürich.

Appendix A. Supplementary material

Supplementary data associated with this article can be found in the online version at <http://dx.doi.org/10.1016/j.ydbio.2016.07.018>.

References

- Ambros, V., 1999. Cell cycle-dependent sequencing of cell fate decisions in *Caenorhabditis elegans* vulva precursor cells. *Development* 126, 1947–1956.
- Berset, T., Hoier, E.F., Battu, G., Canevascini, S., Hajnal, A., 2001. Notch inhibition of RAS signaling through MAP kinase phosphatase LIP-1 during *C. elegans* vulval development. *Science* 291, 1055–1058. <http://dx.doi.org/10.1126/science.1055642>.
- Brenner, S., 1974. The genetics of *Caenorhabditis elegans*. *Genetics* 77, 71–94.
- Brodigan, T.M., Liu, J.L., Park, M., Kipreos, E.T., Krause, M., 2003. Cyclin E expression during development in *Caenorhabditis elegans*. *Dev. Biol.* 254, 102–115.
- Celetti, A., Barba, P., Cillo, C., Rotoli, B., Boncinelli, E., Magli, M.C., 1993. Characteristic patterns of HOX gene expression in different types of human leukemia. *Int. J. Cancer* 53, 237–244.
- Cheng, M., Olivier, P., Diehl, J.A., Fero, M., Roussel, M.F., Roberts, J.M., Sherr, C.J., 1999. The p21(Cip1) and p27(Kip1) CDK “inhibitors” are essential activators of cyclin d-dependent kinases in murine fibroblasts. *EMBO J.* 18, 1571–1583. <http://dx.doi.org/10.1093/emboj/18.6.1571>.
- Clark, S., Chisholm, A., Horvitz, H., 1993. Control of cell fates in the central body region of *C. elegans* by the homeobox gene *lin-39*. *Cell* 74, 43–55.
- Clayton, J.E., van den Heuvel, S.J.L., Saito, R.M., 2008. Transcriptional control of cell-cycle quiescence during *C. elegans* development. *Dev. Biol.* 313, 603–613. <http://dx.doi.org/10.1016/j.ydbio.2007.10.051>.
- Cohn, M.J., Patel, K., Krumlauf, R., Wilkinson, D.G., Clarke, J.D., Tickle, C., 1997. Hox9 genes and vertebrate limb specification. *Nature* 387, 97–101. <http://dx.doi.org/10.1038/387097a0>.
- Dickinson, D.J., Ward, J.D., Reiner, D.J., Goldstein, B., 2013. Engineering the *Caenorhabditis elegans* genome using Cas9-triggered homologous recombination. *Nat. Methods* 10, 1028–1034. <http://dx.doi.org/10.1038/nmeth.2641>.
- Eisenmann, D.M., 2005. Wnt signaling. *WormBook*, 1–17. <http://dx.doi.org/10.1895/wormbook.1.7.1>.
- Eisenmann, D.M., Maloof, J.N., Simske, J.S., Kenyon, C., Kim, S.K., 1998. The Beta-catenin Homolog BAR-1 and LET-60 Ras coordinately regulate the Hox gene *lin-39* during *Caenorhabditis elegans* vulval development. *Development* 125, 3667–3680.
- Farooqui, S., Pellegrino, M.W., Rimann, I., Morf, M.K., Müller, L., Fröhli, E., Hajnal, A., 2012. Coordinated lumen contraction and expansion during vulval tube morphogenesis in *Caenorhabditis elegans*. *Dev. Cell* 23, 494–506. <http://dx.doi.org/10.1016/j.devcel.2012.06.019>.
- Ferguson, E.L., Horvitz, H.R., 1985. Identification and characterization of 22 genes that affect the vulval cell lineages of the nematode *Caenorhabditis elegans*. *Genetics* 110, 17–72.
- Frøkjær-Jensen, C., Davis, M.W., Hopkins, C.E., Newman, B.J., Thummel, J.M., Olesen, S.-P., Grunnet, M., Jørgensen, E.M., 2008. Single-copy insertion of transgenes in *Caenorhabditis elegans*. *Nat. Genet.* 40, 1375–1383. <http://dx.doi.org/10.1038/ng.248>.
- Gleason, J.E., Alex Hajnal, C.W.S.K.K., Fay, D.S., Yoo, A.S., Kishore, R.S., Aroian, R.V., Berset, T., Han, M., Bais, C., Koga, M., Sundaram, M.V., Horvitz, H.R., Greenwald, I., Mendel, J.E., Ohshima, Y., Sternberg, P.W., 2000. Mutations in *cye-1*, a *Caenorhabditis elegans* cyclin E homolog, reveal coordination between cell-cycle control and vulval development. *Development* 127, 4049–4060.
- Guerry, F., Marti, C.-O., Zhang, Y., Moroni, P.S., Jaquière, E., Müller, F., 2007. The Mi-2 nucleosome-remodeling protein LET-418 is targeted via LIN-1/ETS to the promoter of *lin-39/Hox* during vulval development in *C. elegans*. *Dev. Biol.* 306, 469–479. <http://dx.doi.org/10.1016/j.ydbio.2007.03.026>.
- Haag, A., Gutierrez, P., Bühler, A., Wälsler, M., Yang, Q., Langouët, M., Kradolfer, D., Fröhli, E., Herrmann, C.J., Hajnal, A., Escobar-Restrepo, J.M., 2014. An in vivo EGF receptor localization screen in *C. elegans* identifies the Ezrin homolog ERM-1 as a temporal regulator of signaling. *PLoS Genet.* 10, e1004341. <http://dx.doi.org/10.1371/journal.pgen.1004341.s007>.
- van den Heuvel, S., 2005. Cell-cycle regulation. *WormBook*, 1–16. <http://dx.doi.org/10.1895/wormbook.1.28.1>.
- Hombria, J., Lovegrove, B., 2003. Beyond homeosis—HOX function in morphogenesis and organogenesis. *Differentiation* 71, 461–476.
- Hong, Y., Roy, R., Ambros, V., 1998. Developmental regulation of a cyclin-dependent kinase inhibitor controls postembryonic cell cycle progression in *Caenorhabditis elegans*. *Development* 125, 3585–3597.

- Hoyos, E., Euling, S., Kim, K., Ambros, V., Milloz, J., Barkoulas, M., Pénigault, J.-B., Munro, E., Félix, M.-A., 1996. Heterochronic genes control cell cycle progression and developmental competence of *C. elegans* vulva precursor cells. *Cell* 84, 667–676.
- Hwang, B.J., Sternberg, P.W., 2004. A cell-specific enhancer that specifies lin-3 expression in the *C. elegans* anchor cell for vulval development. *Development* 131, 143–151. <http://dx.doi.org/10.1242/dev.00924>.
- Jacobs, D., Beitel, G.J., Clark, S.G., Horvitz, H.R., Kornfeld, K., 1998. Gain-of-function mutations in the *Caenorhabditis elegans* lin-1 ETS gene identify a C-terminal regulatory domain phosphorylated by ERK MAP kinase. *Genetics* 149, 1809.
- Koh, K., Peyrot, S.M., Wood, C.G., Wagmeister, J.A., Maduro, M.F., Eisenmann, D.M., Rothman, J.H., 2002. Cell fates and fusion in the *C. elegans* vulval primordium are regulated by the EGL-18 and ELT-6 GATA factors – apparent direct targets of the LIN-39 Hox protein. *Development* 129, 5171–5180.
- Lewis, E.B., 1978. A gene complex controlling segmentation in *Drosophila*. *Nature* 276, 565–570.
- Mahfooz, N.S., Li, H., Popadić, A., 2004. Differential expression patterns of the hox gene are associated with differential growth of insect hind legs. *Proc. Natl. Acad. Sci. USA* 101, 4877–4882. <http://dx.doi.org/10.1073/pnas.0401216101>.
- Mallof, J., Kenyon, C., 1998. The Hox gene lin-39 is required during *C. elegans* vulval induction to select the outcome of Ras signaling. *Development* 125, 181–190.
- Mann, R.S., Affolter, M., 1998. Hox proteins meet more partners. *Curr. Opin. Genet. Dev.* 8, 423–429.
- Mello, C.C., Kramer, J.M., Stinchcomb, D., Ambros, V., 1991. Efficient gene transfer in *C. elegans*: extrachromosomal maintenance and integration of transforming sequences. *EMBO J.* 10, 3959–3970.
- Miller, L.M., Gallegos, M.E., Morisseau, B.A., Kim, S.K., 1993. lin-31, a *Caenorhabditis elegans* HNF-3/fork head transcription factor homolog, specifies three alternative cell fates in vulval development. *Genes Dev.* 7, 933–947.
- Niu, W., Lu, Z.J., Zhong, M., Sarov, M., Murray, J.I., Brdlik, C.M., Janette, J., Chen, C., Alves, P., Preston, E., Slightam, C., Jiang, L., Hyman, A.A., Kim, S.K., Waterston, R.H., Gerstein, M., Snyder, M., Reinke, V., 2011. Diverse transcription factor binding features revealed by genome-wide ChIP-seq in *C. elegans*. *Genome Res.* 21, 245–254. <http://dx.doi.org/10.1101/gr.114587.110>.
- Nusser-Stein, S., Beyer, A., Rimann, I., Adamczyk, M., Piterman, N., Hajnal, A., Fisher, J., 2012. Cell-cycle regulation of NOTCH signaling during *C. elegans* vulval development. *Mol. Syst. Biol.* 8. <http://dx.doi.org/10.1038/msb.2012.51>.
- Park, M., Krause, M.W., 1999. Regulation of postembryonic G(1) cell cycle progression in *Caenorhabditis elegans* by a cyclin D/CDK-like complex. *Development* 126, 4849–4860.
- Pellegrino, M.W., Farooqui, S., Fröhli, E., Rehrauer, H., Kaeser-Pebner, S., Müller, F., Gasser, R.B., Hajnal, A., 2011. LIN-39 and the EGFR/RAS/MAPK pathway regulate *C. elegans* vulval morphogenesis via the VAB-23 zinc finger protein. *Development* 138, 4649–4660. <http://dx.doi.org/10.1242/dev.071951>.
- Podbilewicz, B., Leikina, E., Sapir, A., Valansi, C., Suissa, M., Shemer, G., Chernomordik, L.V., 2006. The *C. elegans* developmental fusogen EFF-1 mediates homotypic fusion in heterologous cells and in vivo. *Dev. Cell* 11, 471–481. <http://dx.doi.org/10.1016/j.devcel.2006.09.004>.
- Regős, Á., Lengyel, K., Takács-Vellai, K., Vellai, T., 2013. Identification of novel cis-regulatory regions from the Notch receptor genes lin-12 and glp-1 of *Caenorhabditis elegans*. *Gene Expr. Patterns* 13, 66–77. <http://dx.doi.org/10.1016/j.gexp.2012.11.002>.
- Rezsohazy, R., Saurin, A.J., Maurel-Zaffran, C., Graba, Y., 2015. Cellular and molecular insights into Hox protein action. *Development* 142, 1212–1227. <http://dx.doi.org/10.1242/dev.109785>.
- Roy, S.H., Clayton, J.E., Holmen, J., Beltz, E., Saito, R.M., 2011. Control of Cdc14 activity coordinates cell cycle and development in *Caenorhabditis elegans*. *Mech. Dev.* 128, 317–326. <http://dx.doi.org/10.1016/j.mod.2011.06.001>.
- Saito, R.M., Perreault, A., Peach, B., Satterlee, J.S., van den Heuvel, S., 2004. The CDC-14 phosphatase controls developmental cell-cycle arrest in *C. elegans*. *Nat. Cell Biol.* 6, 777–783. <http://dx.doi.org/10.1038/ncb1154>.
- Schiedlmeier, B., Santos, A.C., Ribeiro, A., Moncaut, N., Lesinski, D., Auer, H., Kornacker, K., Ostertag, W., Baum, C., Mallo, M., Klump, H., 2007. HOXB4's road map to stem cell expansion. *Proc. Natl. Acad. Sci. USA* 104, 16952–16957. <http://dx.doi.org/10.1073/pnas.0703082104>.
- Schindelin, J., Arganda-Carreras, I., Frise, E., Kaynig, V., Longair, M., Pietzsch, T., Preibisch, S., Rueden, C., Saalfeld, S., Schmid, B., Tinevez, J.-Y., White, D.J., Hartenstein, V., Eliceiri, K., Tomancak, P., Cardona, A., 2012. Fiji: an open-source platform for biological-image analysis. *Nat. Methods* 9, 676–682. <http://dx.doi.org/10.1038/nmeth.2019>.
- Schindler, A.J., Sherwood, D.R., 2012. Morphogenesis of the *Caenorhabditis elegans* vulva. *Wiley Interdiscip. Rev. Dev. Biol.* 2, 75–95. <http://dx.doi.org/10.1002/wdev.87>.
- Schmid, T., Hajnal, A., 2015. Signal transduction during *C. elegans* vulval development: a NeverEnding story. *Curr. Opin. Genet. Dev.* 32, 1–9. <http://dx.doi.org/10.1016/j.gde.2015.01.006>.
- Shaye, D.D., Greenwald, I., 2002. Endocytosis-mediated downregulation of LIN-12/Notch upon Ras activation in *Caenorhabditis elegans*. *Nature* 420, 686–690. <http://dx.doi.org/10.1038/nature01234>.
- Shemer, G., Podbilewicz, B., 2002. LIN-39/Hox triggers cell division and represses EFF-1/fusogen-dependent vulval cell fusion. *Genes Dev.* 16, 3136–3141. <http://dx.doi.org/10.1101/gad251202>.
- Soulier, J., Clappier, E., Cayuela, J.-M., Regnault, A., García-Peydró, M., Dombret, H., Baruchel, A., Toribio, M.-L., Sigaux, F., 2005. HOXA genes are included in genetic and biologic networks defining human acute T-cell leukemia (T-ALL). *Blood* 106, 274–286. <http://dx.doi.org/10.1182/blood-2004-10-3900>.
- Sternberg, P.W., 2005. Vulval development. *WormBook*, 1–28. <http://dx.doi.org/10.1895/wormbook.1.6.1>.
- Sundaram, M.V., 2006. RTK/Ras/MAPK signaling. *WormBook*, 1–19. <http://dx.doi.org/10.1895/wormbook.1.80.1>.
- Szabó, E., Hargitai, B., Regős, Á., Tihanyi, B., Barna, J., Borsos, É., Takács-Vellai, K., Vellai, T., 2009. TRA-1/GLI controls the expression of the Hox gene lin-39 during *C. elegans* vulval development. *Dev. Biol.* 330, 339–348. <http://dx.doi.org/10.1016/j.ydbio.2009.04.005>.
- Takács-Vellai, K., Vellai, T., Chen, E.B., Zhang, Y., Guerry, F., Stern, M.J., Müller, F., 2007. Transcriptional control of Notch signaling by a HOX and a PBX/EXD protein during vulval development in *C. elegans*. *Dev. Biol.* 302, 661–669. <http://dx.doi.org/10.1016/j.ydbio.2006.09.049>.
- Tan, P.B., Lackner, M.R., Kim, S.K., 1998. MAP kinase signaling specificity mediated by the LIN-1 Ets/LIN-31 WH transcription factor complex during *C. elegans* vulval induction. *Cell* 93, 569–580.
- Thummel, R., Ju, M., Sarras, M.P., Godwin, A.R., 2007. Both Hoxc13 orthologs are functionally important for zebrafish tail fin regeneration. *Dev. Genes Evol.* 217, 413–420. <http://dx.doi.org/10.1007/s00427-007-0154-3>.
- Trinkaus, J.P., 1984. *Cells into Organs*. N. J., Prentice Hall, Englewood Cliffs.
- Wagmeister, J.A., Gleason, J.E., Eisenmann, D.M., 2006a. Transcriptional upregulation of the *C. elegans* Hox gene lin-39 during vulval cell fate specification. *Mech. Dev.* 123, 135–150. <http://dx.doi.org/10.1016/j.mod.2005.11.003>.
- Wagmeister, J.A., Miley, G.R., Morris, C.A., Gleason, J.E., Miller, L.M., Kornfeld, K., Eisenmann, D.M., 2006b. Identification of cis-regulatory elements from the *C. elegans* Hox gene lin-39 required for embryonic expression and for regulation by the transcription factors LIN-1, LIN-31 and LIN-39. *Dev. Biol.* 297, 550–565. <http://dx.doi.org/10.1016/j.ydbio.2006.05.008>.
- Yang, L., Sym, M., Kenyon, C., 2005. The roles of two *C. elegans* HOX co-factor orthologs in cell migration and vulva development. *Development* 132, 1413–1428. <http://dx.doi.org/10.1242/dev.01569>.
- Yoo, A.S., Bais, C., Greenwald, I., 2004. Crosstalk between the EGFR and LIN-12/Notch pathways in *C. elegans* vulval development. *Science* 303, 663–666. <http://dx.doi.org/10.1126/science.1091639>.
- Zhang, X., Greenwald, I., 2011. Spatial regulation of lag-2 transcription during vulval precursor cell fate patterning in *Caenorhabditis elegans*. *Genetics* 188, 847–858. <http://dx.doi.org/10.1534/genetics.111.128389>.